Numerical simulation of magnons

Sondre Duna Lundemo†
Department of Physics, Norwegian University of Science and Technology, Trondheim
Norway

TFY4235 - Computational physics
(*Last updated on March 4, 2021*)

†sondre@duna.no

Contents

PART I

Introduction

1 Theoretical background

Hamiltonian

$$H = -\frac{1}{2}\sum_{j,k}^{N} J_{jk}\mathbf{S}_j \cdot \mathbf{S}_k - d_z \sum_{j=1}^{N}(S_{j,z})^2 - \mu \sum_{j=1}^{N}\mathbf{B}_j \cdot \mathbf{S}_j \tag{1}$$

Landau-Lifshitz-Gilbert equation

$$\partial_t \mathbf{S}_j = \frac{-\gamma}{\mu(1+\alpha^2)}\left[\mathbf{S}_j \times \mathbf{H}_j + \alpha \mathbf{S}_j \times (\mathbf{S}_j \times \mathbf{H}_j)\right] \tag{2}$$

where

$$\mathbf{H}_j = -\frac{\partial H}{\partial \mathbf{S}_j} + \boldsymbol{\xi}_j. \tag{3}$$

In the absence of noise we can find an explicit relation for the effective field $\mathbf{H}_j$ in (3). This can be done by noting that

$$\begin{aligned}
-\frac{\partial H}{\partial \mathbf{S}_j} &= \frac{1}{2}\sum_{i,k}^{N} J_{ik}\frac{\partial}{\partial \mathbf{S}_j}\left(\mathbf{S}_i \cdot \mathbf{S}_k\right) + d_z \sum_{i=1}^{N}\frac{\partial}{\partial \mathbf{S}_j}(\mathbf{S}_i \cdot \mathbf{e}_z)^2 + \mu \sum_{i=1}^{N}\frac{\partial}{\partial \mathbf{S}_j}\mathbf{B}_i \cdot \mathbf{S}_i \\
&= \frac{1}{2}\sum_{i,k}^{N} J_{ik}\left(\delta_{ij}\mathbf{S}_k + \delta_{jk}\mathbf{S}_i\right) + d_z \sum_{i=1}^{N} 2\delta_{ij}(\mathbf{S}_i \cdot \mathbf{e}_z)\mathbf{e}_z + \mu \sum_{i=1}^{N}\mathbf{B}_i\delta_{ij} \\
&= \sum_{i=1}^{N} J_{ij}\mathbf{S}_i + 2d_z S_{j,z}\mathbf{e}_z + \mu\mathbf{B} \\
&= \sum_{i\in\mathcal{N}_j} J_{ij}\mathbf{S}_i + 2d_z S_{j,z}\mathbf{e}_z + \mu\mathbf{B},
\end{aligned}$$

where we in the last transition have made further simplifications by only performing the sum over the nearest neighbours $\mathcal{N}_j$ of j. Using this expression we might rewrite the LLG in (2) as

$$\begin{aligned}
\partial_t \mathbf{S}_j = \frac{-\gamma}{\mu(1+\alpha^2)}\Bigg[&\mathbf{S}_j \times \left(\sum_{i\in\mathcal{N}_j} J_{ij}\mathbf{S}_i + 2d_z S_{j,z}\mathbf{e}_z + \mu\mathbf{B}\right) \\
&+\alpha\mathbf{S}_j \times \left[\mathbf{S}_j \times \left(\sum_{i\in\mathcal{N}_j} J_{ij}\mathbf{S}_i + 2d_z S_{j,z}\mathbf{e}_z + \mu\mathbf{B}\right)\right]\Bigg].
\end{aligned}$$

PART II

Code overview

2 General structure

3 Remarks on performance

PART III

Results and discussion

4 Single spin

4.1 Precession of spin in uniform magnetic field

We simulate the time evolution of a single spin $\mathbf{S}$ in the presence of a uniform magnetic field $\mathbf{B} = (0, 0, B_0)^T$ in the $\mathbf{e}_z$-direction. The components of the spin at equidistant time steps during one period are shown in figure 1. As expected, we see that the spin precesses around the effective field $\mathbf{H}$, which in this case is given by

$$\mathbf{H} = -\frac{\partial H}{\partial \mathbf{S}} = \frac{\partial}{\partial \mathbf{S}} (\mu \mathbf{B} \cdot \mathbf{S}) = \mu \mathbf{B},$$

in the absence of damping and anisotropy.

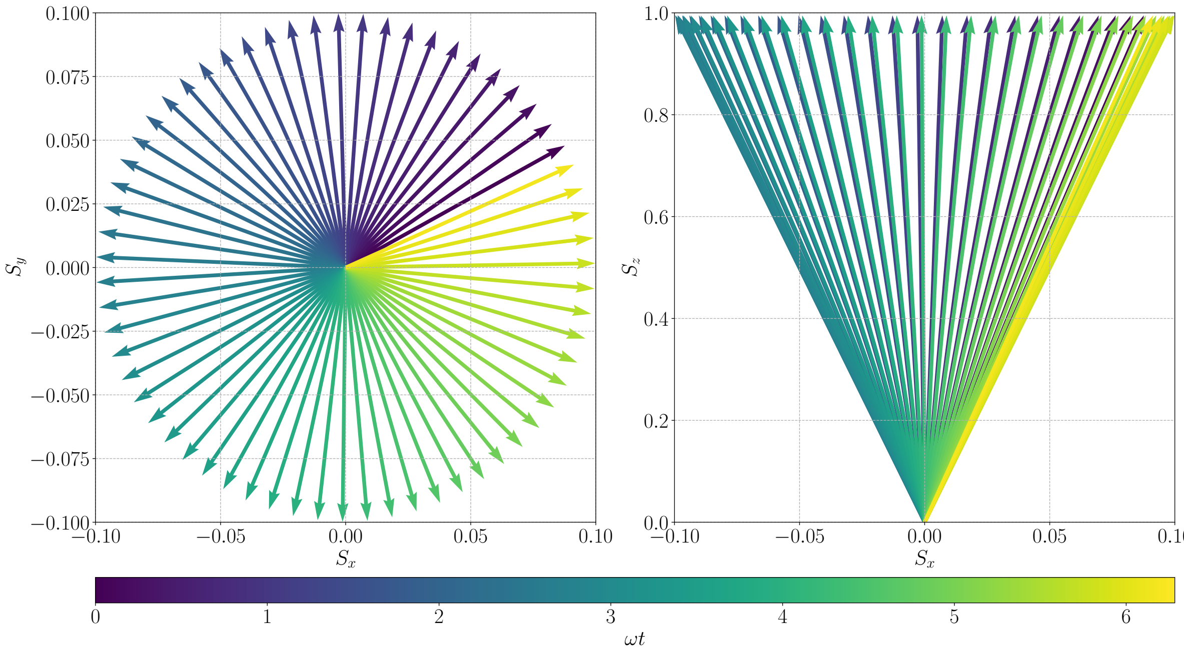

Figure 1: The figure shows the x and y component of the spin during one period in a uniform magnetic field without further interactions.

In this particular case, we can easily find an analytical solution to compare with. The LLG-equation reads

$$\partial_t \mathbf{S} = -\gamma \mathbf{S} \times \mathbf{B}.$$

As $\mathbf{B} = (0, 0, B_0)^T$,

$$\mathbf{S} \times \mathbf{B} = (S_y \mathbf{e}_x - S_x \mathbf{e}_y) B_0.$$

Thus, we have two equations

$$\begin{cases} \partial_t S_x = -\gamma B_0 S_y \\ \partial_t S_y = \gamma B_0 S_x. \end{cases} \tag{4}$$

which are easily solved by differentiating both with respect to t, and then substituting the first order derivatives on the right hand side by the corresponding expressions in 4.

$$\begin{cases} \partial_t^2 S_x = -\gamma B_0 \partial_t S_y \\ \partial_t^2 S_y = \gamma B_0 \partial_t S_x. \end{cases} \tag{5}$$

This yields the two equations

$$\ddot{S}_x = -\left(\gamma B_0\right)^2 S_x \quad ; \quad \ddot{S}_y = -\left(\gamma B_0\right)^2 S_y, \tag{6}$$

which have solutions

$$S_x(t) = S_x(0)\cos\left(\omega t\right) - S_y(0)\sin\left(\omega t\right) \tag{7}$$
$$S_y(t) = S_y(0)\cos\left(\omega t\right) + S_x(0)\sin\left(\omega t\right), \tag{8}$$

with the frequency $\omega = \gamma B_0$. When comparing the exact solution with the numerical estimate obtained through integrating the LLG-equation with Heun's method, the trajectories of S_x and S_y are as shown in figure 2.

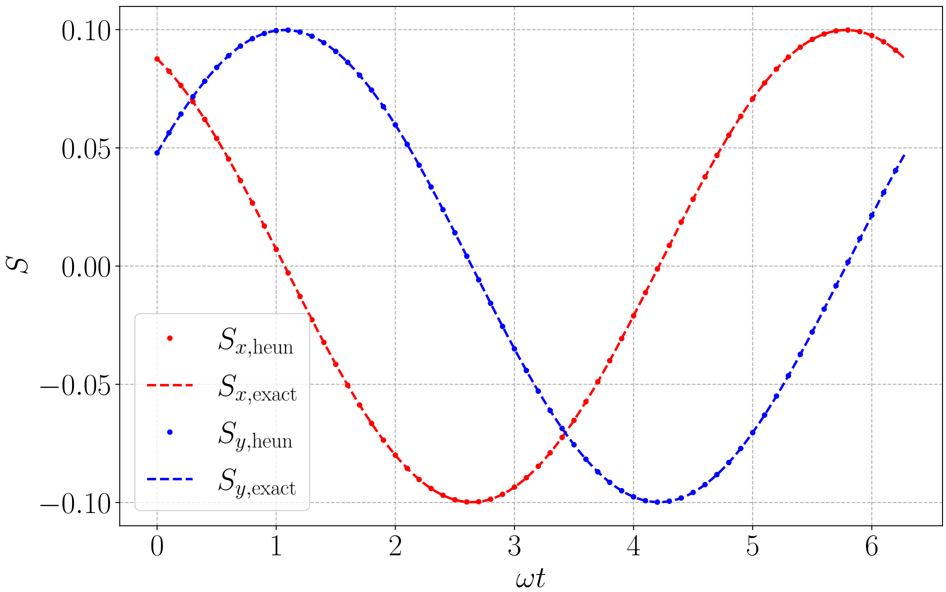

Figure 2: The plot shows the exact solution given in (7) and (8) compared with the numerical solution sampled at every tenth step to be able to distinguish the paths.

It is perhaps more enlightening to consider the pointwise difference of the exact and numerical solution. This is shown in figure 3. The figure shows that the deviations locally oscillate, and that the absolute global deviations increase with time as we'd expect. Further considerations on the deviations are considered in 4.2.

4.2 Error analysis

For the error analysis, I choose 10 logarithmically spaced step-lengths from 10^{-5} to 10^{-1}. As a measure of the *global error*, that is the cumulated error over one period. The error as a function of step length is shown in figure 4.

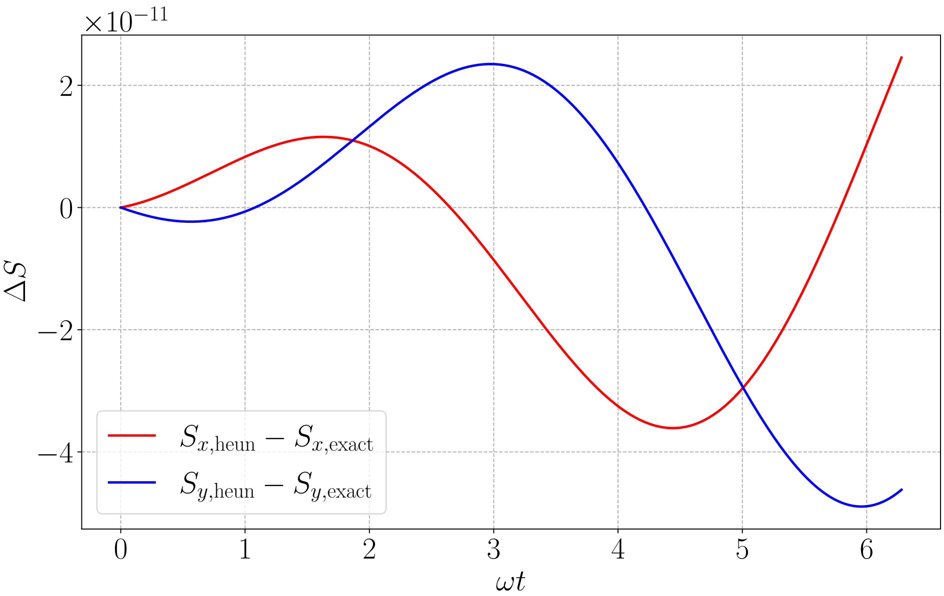

Figure 3: The plot shows the difference between the exact solutions given in (7) and (8), and the numerical solutions over one period.

Since Heun's method is of second order, we would expect its slope in a log-log plot to be roughly 2. However, as demonstrated in figure 4, the slope is slightly less than 2. This is due to FIND REASON FOR THIS. In figure 5 we have plotted the errors for Euler's method for the same step lengths. This plot clearly demonstrates the well known fact that Euler's method is of order 1.

4.3 Damped precession of spin in magnetic field

Next, we include damping in the model. This amounts to setting $\alpha \neq 0$. The plots of the trajectories in the x and y direction for three different damped cases is shown in figure 6. The damping lifetime $\tau = \frac{1}{\alpha\omega}$.

5 The spin chain

5.1 Ground states

5.2 The magnon

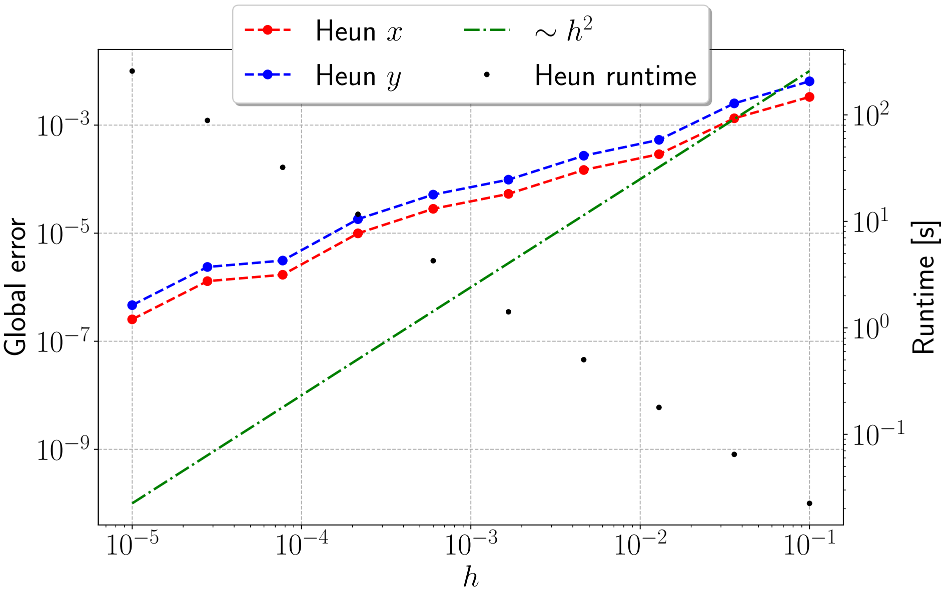

Figure 4: Error as a function of step length for Heun's method.

PART IV

Conclusion

References

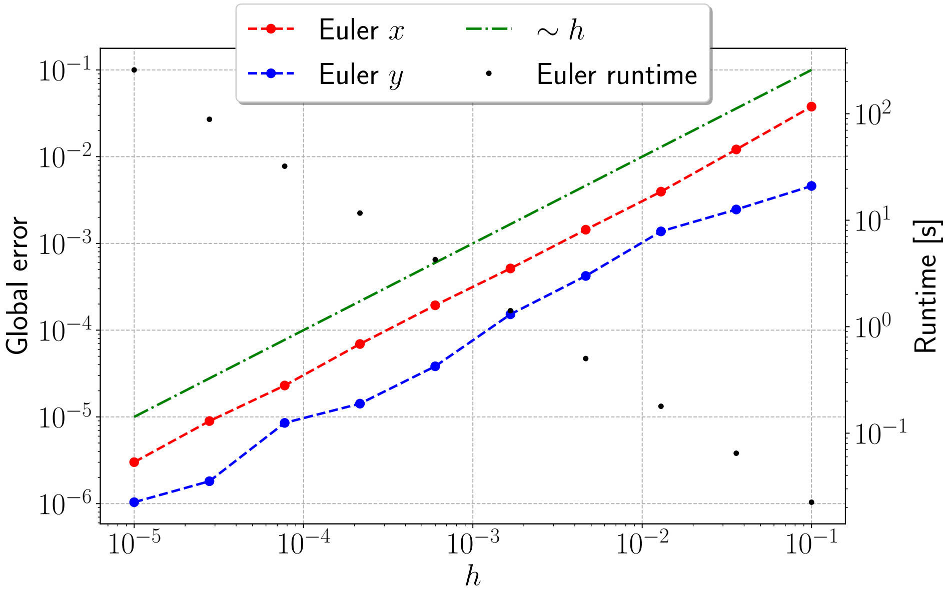

Figure 5: Error as a function of step length for Euler's method.

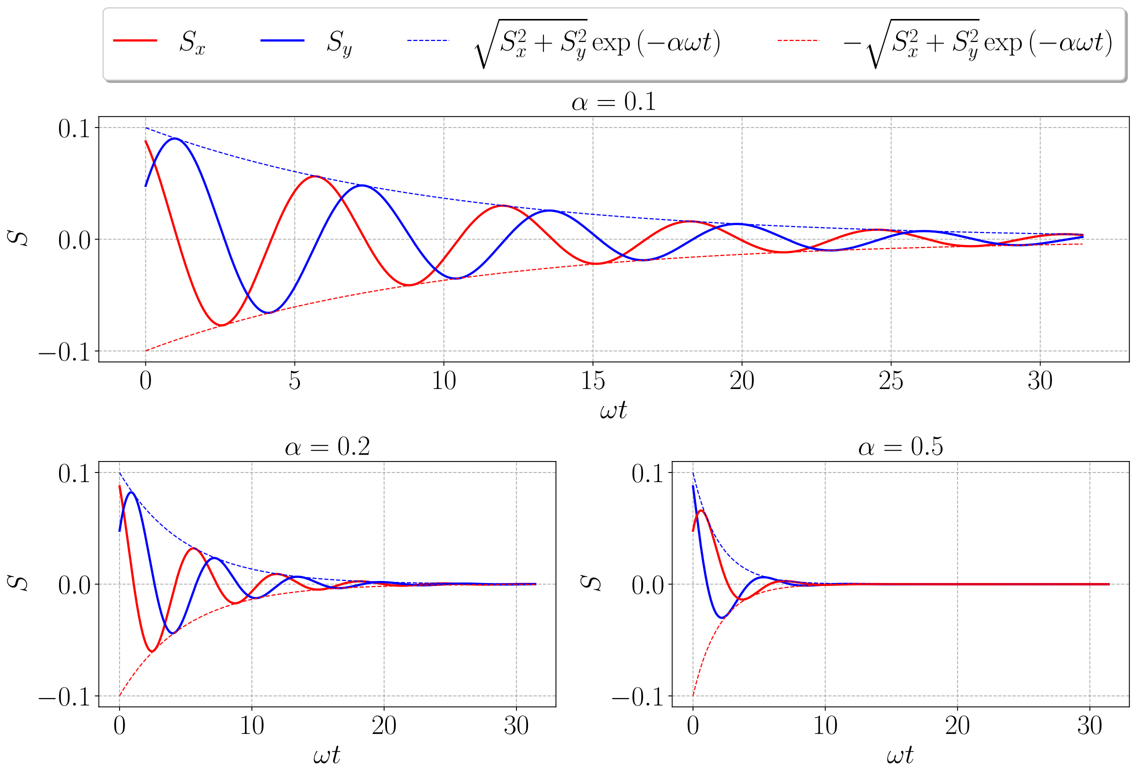

Figure 6: Three different damped precessions.